

Simulated Sunlight-Induced Photodegradations of Triasulfuron and Cinosulfuron in Aqueous Solutions

E. VULLIET,[†] C. EMMELIN,[†] M. F. GRENIER-LOUSTALLOT,[‡] O. PAÏSSÉ,[‡] AND
 J. M. CHOVELON^{*,†}

LACE, Laboratoire d'Application de la Chimie à l'Environnement, UMR 5634,
 CNRS 43 bld du 11 novembre 1918, 69622 Villeurbanne Cedex, France, and SCA Service Central
 D'analyse, USR 059 CNRS, Echangeur de Solaise, B.P. 22, 69390 Vernaison, France

To elucidate the photochemical behavior of two sulfonylureas (cinosulfuron and triasulfuron) for which the chemical formulas are relatively close, their photodegradation was studied in water. All experiments were carried out under laboratory conditions using a xenon arc lamp as the source of radiation to simulate environmental conditions. Polychromatic quantum efficiencies were calculated to determine the photochemical pesticide lifetimes at pH 7, and a comparison with hydrolysis lifetimes has been performed. The results obtained showed clearly that at pH 7, photodegradation becomes a more important pathway than chemical degradation. HPLC-DAD was used to study the kinetics for both sulfonylureas and their photoproducts, whereas HPLC-MS (ESI in positive and negative modes) was used to identify photoproducts. These results suggest that the photodegradation of these two sulfonylureas proceeds via a number of reaction pathways: (1) cleavage of the sulfonylurea bridge; (2) desulfonylation, which can proceed either by a carbon–sulfur cleavage or a nitrogen–sulfur cleavage; (3) O-demethylation of methoxy moieties present on the triazine ring; and (4) O-dealkylation of benzene derivatives. In addition, it was found that the desulfonylation represented the main step and that it was wavelength dependent.

KEYWORDS: Cinosulfuron; triasulfuron; photodegradation; quantum efficiency; HPLC-MS analysis

INTRODUCTION

Since the early 1980s, there has been a dramatic increase in the number of as well as the use of sulfonylurea herbicides to control broadleaf weeds and some grasses in cereal crops. Some of the reasons for their rapid and good acceptance include low application rates (~2–75 g/ha), good crop selectivity, and very low acute and chronic animal toxicity.

Their mode of action consists of the inhibition of acetolactate synthase (ALS), a key enzyme in the biosynthetic pathway of branched-chain amino acids (leucine, isoleucine, and valine) in the plant.

Although it is claimed that chemical hydrolysis and microbial degradation represent the main degradation pathways of sulfonylureas (1, 2), several papers indicate that photodegradation is an alternative pathway to chemical hydrolysis (3–6). Indeed, the chemical degradation rates of sulfonylureas are pH dependent, and generally these compounds are more susceptible to chemical hydrolysis at acidic rather than at neutral or weakly basic pH (7, 8). Therefore, we can easily imagine that at neutral pH, photodegradation can become an important pathway. In addition, it is known that photodegradation processes can

accelerate chemical hydrolysis (photoassisted reaction) or form new products. In this context, photochemical investigation may contribute to a better understanding of pesticide behavior in the environment.

This paper reports on the photochemical behavior in water of two sulfonylureas (SAs), cinosulfuron (CS) and triasulfuron (TS). The quantum efficiency has also been calculated and the kinetics followed. The different photoproducts have been identified and compared with those obtained in the literature for chemical hydrolysis, and a pathway of photochemical degradation has been proposed.

MATERIALS AND METHODS

Chemicals. Cinosulfuron [CAS Registry No. 94593-91-6, 1-(4,6-dimethoxy-1,3,5-triazin-2-yl)-3-[(2-methoxyethoxy)phenyl]urea] and triasulfuron [CAS Registry No. 82097-50-5, [2-(6-methoxy-4-methyl-1,3,5-triazin-2-yl)-1-[2-(2-chloroethoxy)phenylsulfonyl]urea]] were purchased from Riedel De Haën and were used as received. Their limits of solubility in water are 815 mg L⁻¹ for CS and 4000 mg L⁻¹ for TS at pH 7 and 25 °C. 2-Amino-4-methoxy-6-methyl-1,3,5-triazine was purchased from Aldrich and (2-chloroethoxy)benzene from Fluka. For photodegradation experiments, pesticides were solubilized in phosphate buffer (K₂HPO₄/KH₂PO₄ 5 × 10⁻³ M), whereas for hydrolysis studies three buffers were used: acetate buffer for pH 5, phosphate buffer for pH 7, and borate buffer for pH 9. The water used for LC mobile phase and buffer preparation was purified with a Millipore system (Milli-Q-50 18 MΩ).

* Author to whom correspondence should be addressed [telephone (33) 04.72.43.26.38; fax (33) 04.72.44.81.14; e-mail chovelon@univ-lyon1.fr].

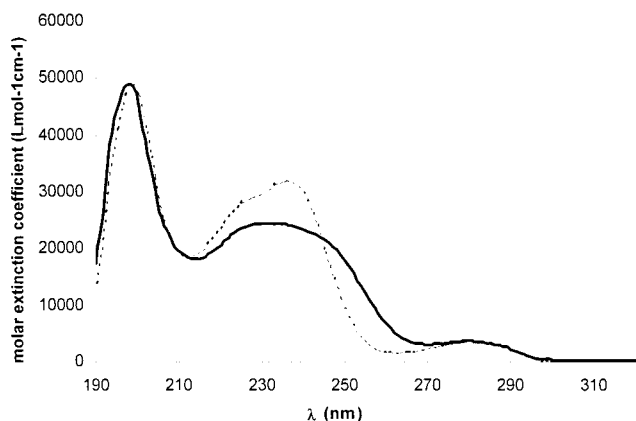
[†] LACE.

[‡] SCA.

Table 1. Rate Constant ($\times 10^2 \text{ h}^{-1}$) for Hydrolysis of Cinosulfuron and Triasulfuron at Different pH Values and in Pure Water

	k_{dark} (CS)	k_{dark} (TS)
pure water	0.01	0.06
pH 5	0.05	0.1
pH 7	NE ^a	0.002
pH 8.9	0.009	0.003

^a Not estimated because the hydrolysis proceeded at a much slower rate.

**Figure 1.** UV spectra of cinosulfuron (---) and triasulfuron (—) in phosphate buffer.**Table 2.** Energy of Singlet (E_{S_1}) and Triplet (E_{T_1}) States

	CS	TS
E_{S_1} (kJ/mol)	408.3	409.7
E_{T_1} (kJ/mol)	302.8	304.4

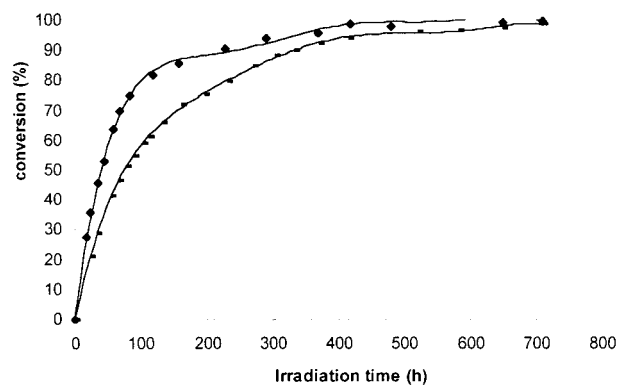
Spectrometer Apparatus. The absorption spectra were recorded with a double-beam UVIKON 930 spectrophotometer (Kontron Instruments), whereas fluorescence and phosphorescence spectra were recorded on a Kontron SFM 25 fluorometer. Fluorescence was measured in a phosphate buffer, whereas phosphorescence was measured in EPA, a mixture made up of isopentane (18%), ethanol (41%), and diethyl ether (41%).

Photodegradation Equipment. A solar simulator (Suntest CPS+, Heraeus), equipped with a 1.5 kW xenon arc lamp, protected with an adequate filter to simulate the solar spectrum between 290 and 800 nm, was used, and the experiments were carried out in ordinary atmosphere at 20 °C.

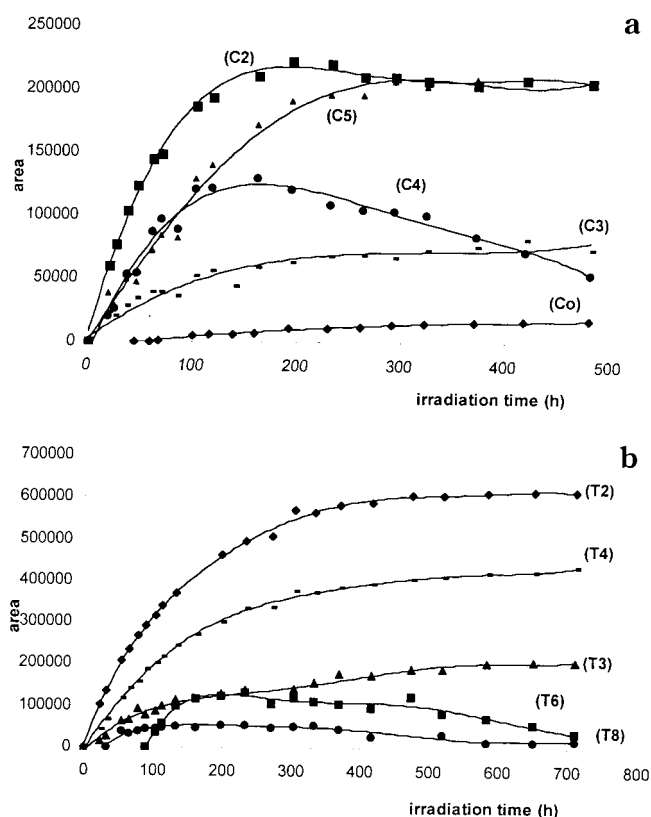
Kinetics of Photodegradation. Phosphate buffer solutions of SAs (0.09 mM for cinosulfuron and 0.01 mM for triasulfuron) were irradiated for 500 and 700 h, respectively. This buffer was chosen as no absorption in the wavelength range studied was found and no shift of absorbance spectrum bands occurred. At selected time intervals, samples were collected and analyzed directly (without preconcentration), using HPLC-DAD.

HPLC Conditions for Kinetic Studies. HPLC analyses were performed with a Shimadzu VP series HPLC system equipped with a photodiode array detector (DAD). A Hypersil BDS C_{18} column (5 μm , 125 \times 4 mm) was used with a gradient elution of (A) methanol and (B) water (pH was set up at 2.80 with phosphoric acid). The gradient used was 95% (B) at $t = 0$, to 50% (B) at $t = 30$ min, and 50% (B) during 10 min. The flow rate was set at 1 mL min^{-1} , and the injection volume was 20 μL .

Photoproduct Identification. A phosphate buffer solution of SAs was irradiated for 150 h, and samples were taken at regular intervals. As photoproducts were obtained at very low concentrations, a preconcentration step was required to perform HPLC-MS analysis. In this context, 5 mL of each sample was extracted on a solid phase extraction

**Figure 2.** Conversion rate of cinosulfuron (◆) and triasulfuron (■) during suntest irradiation.**Table 3.** Triasulfuron and Cinosulfuron Kinetic Data and Quantum Efficiencies Obtained in Water

	k_{suntest} (h^{-1})	$t_{1/2, \text{suntest}}$ (h)	Φ molecules/ photon	τ_{sunlight} lifetime (days)	$t_{1/2, \text{sunlight}}$ (days)
CS	3.65×10^{-2}	19	0.071	25	17.3
TS	1.53×10^{-2}	45	0.079	30	20.8

**Figure 3.** Evolution of principal photoproducts during (a) cinosulfuron and (b) triasulfuron suntest irradiation. In these figures, (C2) and (T2) areas were divided by 10 and 3, respectively. Area determination at $\lambda = 220$ nm.

(SPE) cartridge Isolute ENV+ (50 mg, 6 mL). The solid phase was first conditioned with 3 mL of methanol and then 6 mL of deionized water. Afterward, the pesticides were eluted with 0.5 mL of methanol and then analyzed by HPLC-MS.

HPLC-MS Identification. The identification of photoproducts was performed using HPLC-MS equipment (Hewlett-Packard HP 1100 series LC-MSD). The stationary phase consisted of a Hypersil HP Elite

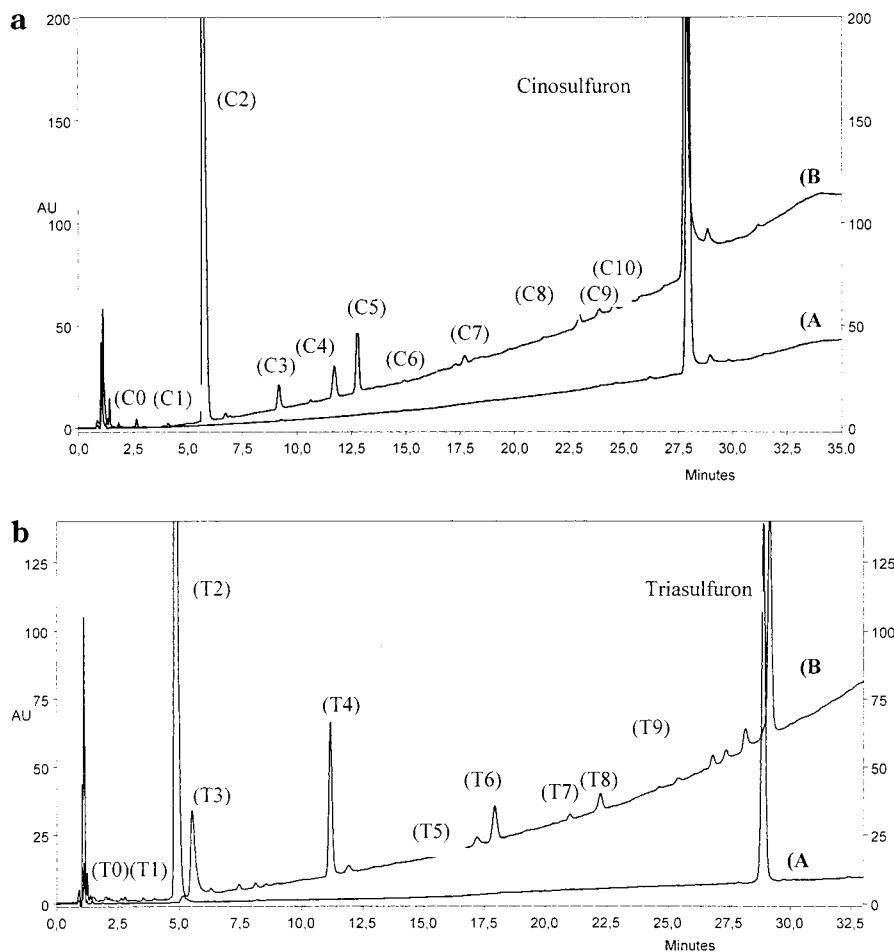


Figure 4. HPLC chromatograms of (A) non-irradiated and (B) irradiated solutions of (a) cinosulfuron and (b) triasulfuron. Irradiation times were 260 and 300 h for CS and TS, respectively. Detection at $\lambda = 220$ nm.

column ($5 \mu\text{m}$, 150×3 mm) and a precolumn thermostated at 40°C . The mobile phases were composed of (A) methanol and (B) 10^{-3} M ammonium formate + formic acid, the pH of which was set to 2.91, and the gradient used was the same as previously described. The injection volume was $2 \mu\text{L}$. MS detection was performed with electrospray ionization (ESI), in positive and negative modes. Operating conditions for nebulization were as follows: capillary potential, 4000 V; auxiliary gas, N_2 ; flow rate, 12 L min^{-1} ; pressure, 55 psig.

Calculation of the Quantum Efficiencies. The quantum efficiencies (Φ) were calculated using custom application software Photon (9), and their values have been defined using the equation

$$\Phi = \frac{dc/dt}{\sum P_{\text{abs}}(t, \lambda)(\Delta\lambda \times 10^3)}$$

where dc denotes the variation of the concentration of the substance for time t and P_{abs} is the absorbed light for the same time in the wavelength range studied. The summation must be performed at appropriate intervals $\Delta\lambda$ (2.5 nm) in the absorption range of the substance.

RESULTS AND DISCUSSION

Aqueous Stability. It is known that the stability of sulfonamide in aqueous solution is markedly influenced by pH (8), which can act on the structures of these compounds. In aqueous solution, SAs exist primarily in neutral form at pH values below their $\text{p}K_{\text{a}}$ values and in anionic form at pH levels above the $\text{p}K_{\text{a}}$ [$\text{p}K_{\text{a}} = 4.7$ for CS and $\text{p}K_{\text{a}} = 4.6$ for TS (10)]. **Table 1**

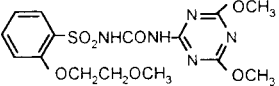
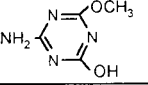
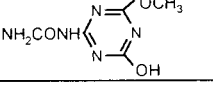
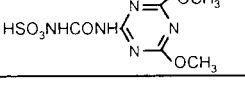
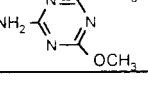
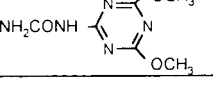
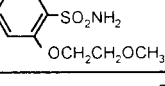
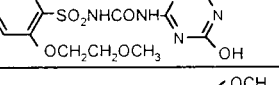
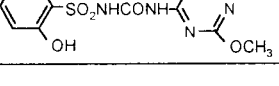
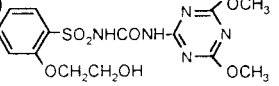
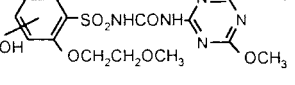
shows the rate constant in the dark at different pH values for CS and TS. From these results we can see that the best stability is obtained for neutral or weakly basic solutions, which is in agreement with those reported by Braschi (8). To reduce chemical hydrolysis, the photolysis experiments were performed at pH 7 (phosphate buffer) for which both selected herbicides are predominantly anionic.

Spectrometric Results. SAs have been found to be composed of two very weakly coupled chromophores (11), the first one corresponding to benzene derivatives and the second to triazine derivatives.

Figure 1 shows the UV spectra of cinosulfuron (CS) and triasulfuron (TS) in phosphate buffer. Both molecules presented three absorption maxima below 290 nm but also a measurable absorption tail up to 300 nm. According to an EC (94/37/CE) directive, phototransformation must be taken into account if the molar extinction coefficient is $>10 \text{ L mol}^{-1} \text{ cm}^{-1}$ for $\lambda \geq 290$ nm. For CS and TS, $\epsilon = 2401$ and $1487 \text{ L mol}^{-1} \text{ cm}^{-1}$, respectively, at $\lambda = 290$ nm, meaning that the photolytic degradation pathway should not be neglected.

The energy of the first excited singlet state and that of the lowest excited triplet state (cf. **Table 2**) were calculated from fluorescence and phosphorescence spectra. Both SAs exhibit a low emission band, at 312 and 310 nm for CS and TS, respectively ($\lambda_{\text{exc}} = 280$ nm for both SAs), in the fluorescence spectra and an emission band at 395 and 393 nm for CS and TS, respectively, in the phosphorescence spectra ($\lambda_{\text{exc}} = 280$ nm for both SAs).

Table 4. Retention Times, Mass Spectra, and UV Data of Photoproducts of Cinosulfuron^a

Compound	T _r (min)	Mass (m/z) ES ⁺	Mass (m/z) ES ⁻	UV data (nm)
CS 	27,8	414 (M+H)⁺, 215 (C ₆ H ₆ (OCH ₂ CH ₂ OCH ₃)S O ₂), 183, 157, 141	412 (M-H)⁻	λ = 286, 222, 195
C0 	2,6	143 (M+H)⁺, 101		λ = 220, 195
C1 	4,1	186 (M+H)⁺, 169 (-OH), 143, 101	184 (M-H)⁻, 141	λ = 219, 192
C2 	5,7	280 (M+H)⁺, 200 (-SO₃), 183, 157	278 (M-H)⁻	λ = 223, 193
C3 	9,2	157 (M+H)⁺, 101, 57		λ = 210, 195
C4	11,7	187 (M+H)⁺, 155, 128, 58		λ = 270, 193, shoulder 220
C5 	12,8	200 (M+H)⁺, 183, 157, 101, 83, 57		λ = 220, 194
C6 	15,0	232 (M+H)⁺, 215 (-NH₂), 102, 88	230 (M-H)⁻	λ = 280, 221, 194
C7 	17,7	400 (M+H)⁺, 313, 215 (C ₆ H ₆ (OCH ₂ CH ₂ OCH ₃)S O ₂), 102, 86	398 (M-H)⁻	λ = 283, 247, 194
C8 	22,9	356 (M+H)⁺, 240, 200 (-C₆H₄SO₃), 183, 157	354 (M-H)⁻, 172	λ = 287, 194 shoulder 220
C9	23,9			λ = 286, 194 shoulder 220
C10 	24,5	400 (M+H)⁺, 282, 266, 201(C₆H₄(SO₂)OCH₂CH₂OH), 183, 157	398 (M-H)⁻, 216	λ = 286, 222, 194
C11-C12-C13 	26,0	430 (M+H)⁺, 428, 296, 294, 183	428 (M-H)⁻, 272, 258, 167	λ = weak
	26,7	430 (M+H)⁺, 414 (-O), 296, 183		λ = 312, 220, 195
	27,4	430 (M+H)⁺, 296, 183	428 (M-H)⁻, 258, 167	λ = 287, 221, 195

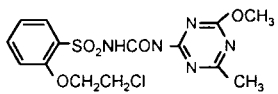
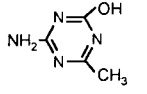
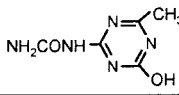
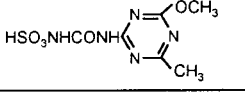
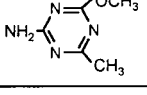
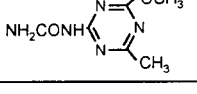
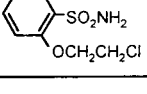
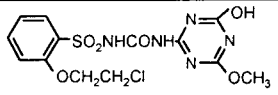
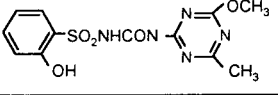
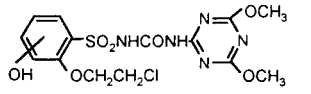
^a Irradiations have been performed with a suntest lamp in a phosphate buffer.

Kinetic Studies. Photodegradation Rates. The kinetic studies were performed at pH 7 using HPLC-DAD analysis. **Figure 2** represents conversion rate curves of both SAs. These results clearly show that the photodegradation is faster for CS than for TS (after 100 h, the conversion rates were 90 and 60% for CS and TS, respectively). A pseudo-first-order reaction for the photodegradation has been found, and kinetic data and quantum

efficiencies for these reactions are given in **Table 3**. Because the hydrolysis rate constants are far lower than the photolysis ones, their contribution will be negligible.

Indeed, the photoreaction values of *k* and *t*_{1/2} cannot be directly compared with those obtained for the hydrolysis because they depend on our individual experimental conditions (lamp power, photoreactor geometry, etc). For direct comparison, the

Table 5. Retention Times, Mass Spectra, and UV Data of Photoproducts of Triasulfuron

Compound	T _r (min)	Mass (m/z) ES ⁺	Mass (m/z) ES ⁻	UV data (nm)
TS 	29,1	404, 402 (M+H) ⁺ , 300, 167, 141	402, 400 (M-H) ⁻	λ = 286, 223, 195
T0 	2	127 (M+H) ⁺		λ = 221, 197
T1 	3,5	170 (M+H) ⁺ , 153 (-OH), 127	168 (M-H) ⁻ , 150 (-H ₂ O), 125	λ = 229, 199
T2 	4,8	264 (M+H) ⁺ , 184 (-SO ₃), 167, 141	262 (M-H) ⁻	λ = 224, 197
T3 	5,5	141 (M+H) ⁺		λ = 216, 193
T4 	11,2	184 (M+H) ⁺ , 167, 141	182 (M-H) ⁻	λ = 222, 193
T5 	15,1	238, 236 (M+H) ⁺ , 221, 219 (-NH ₂), 121		λ = 274, 219, 194
T6	18,0	-	-	λ = 274, 194, shoulder 225
T7 	21,0	390, 388 (M+H) ⁺ , 302, 300, 286, 284, 127	-	λ = 275, 194
T8 	22,2	340 (M+H) ⁺ , 167, 163, 141		λ = 279, 194
T9-T10 	26,8	420, 418 (M+H) ⁺ ,	418, 416 (M-H) ⁻	λ = 291, 194
	27,3	420, 418 (M+H) ⁺ , 318, 316, 300	418, 416 (M-H) ⁻	λ = 278, 194

^a Irradiations have been performed with a suntest lamp in a phosphate buffer.

photolytic parameters under sunlight should be assessed. Such an assessment is possible if the quantum efficiency, the molar extinction coefficient, and the intensity of the solar spectrum in a given area are taken into account. [Zepp and Cline (12) give the intensity of the solar spectrum in North America.] In these conditions, the lifetime can be calculated by the following equation (a solution of low absorbance is required, in which the absorbed light intensity is proportional to the concentration)

$$\tau = \frac{1}{\Phi k_a}$$

where τ denotes the lifetime and k_a is the pseudo-first-order rate constant of direct photolysis in the range of wavelength (290–800 nm) studied and for the outset of the experiment (degradation rate < 8 h). Due to the short period of time selected

and the very low hydrolysis values, k_a can be expressed as

$$k_a = \sum 2.303 \times 10^3 [Po(\lambda)\Delta\lambda\epsilon(\lambda)]$$

where $Po(\lambda)$ represents the solar intensity for wavelength λ [table in Zepp and Cline (12)] and $\epsilon(\lambda)$ the molar extinction coefficient at these wavelengths.

Table 3 summarizes these results, which can be compared to those obtained from the chemical degradation. For example, for TS at pH 7, Brashi et al. (8) have found a half-life of 422 days, Weiss et al. (13) have not estimated it as it proceeded at a much slower rate, and from our own experiments a value of 1444 days has been found.

These results confirm that for neutral pH, direct photodegradation becomes a more important pathway than for pure chemical degradation.

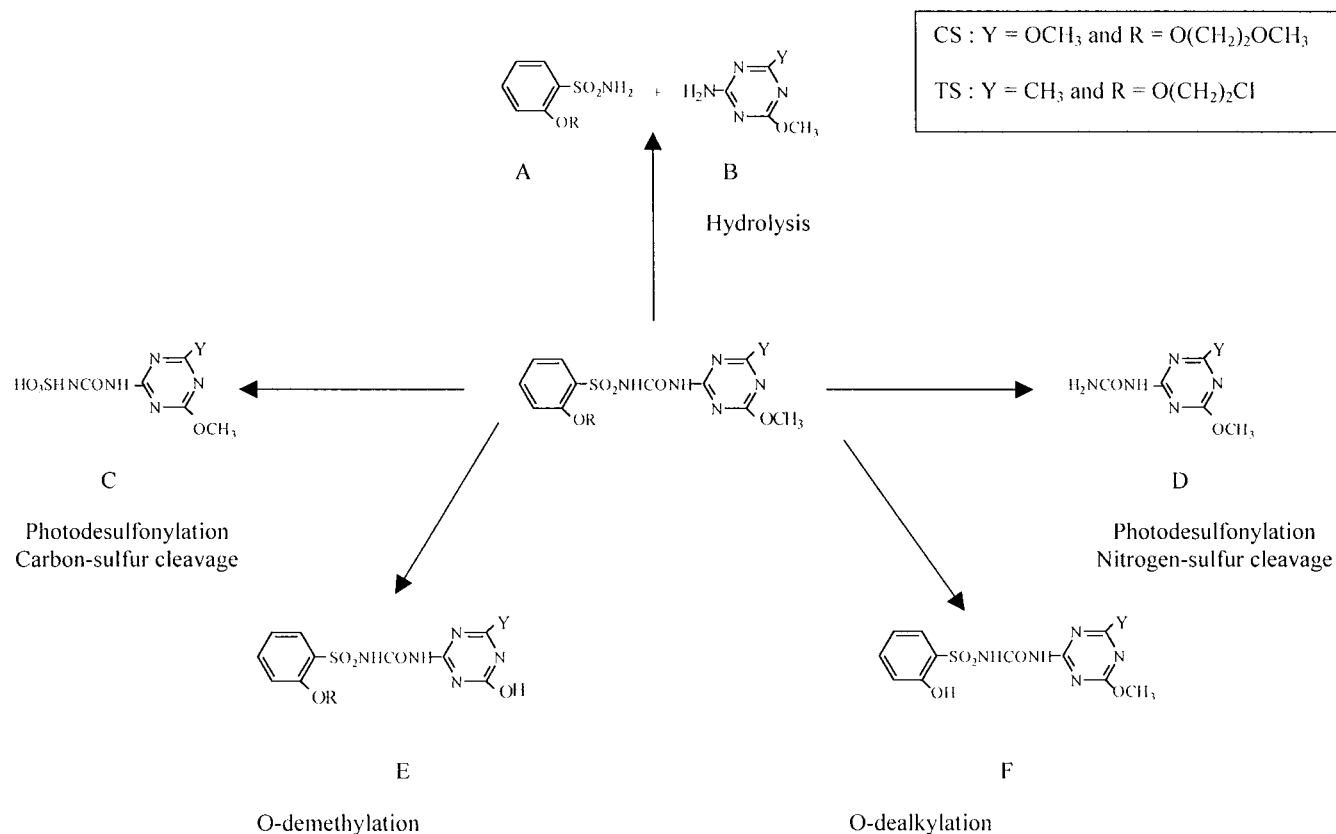


Figure 5. General scheme of photodegradation for CS and TS.

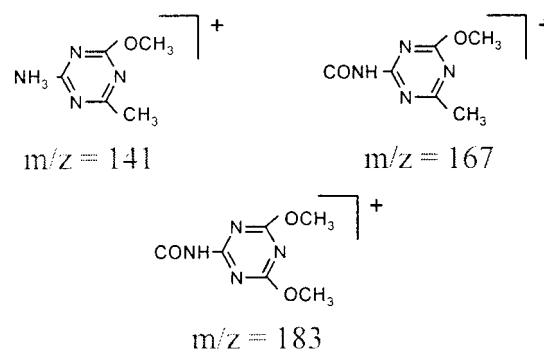
Kinetics of the Main Photoproducts. Figure 3 represents kinetic curves of the five main photoproducts. For both SAs, only the more representative photoproducts are shown, although others have also been identified (cf. Tables 4 and 5). Among them, certain are only intermediates as they will in turn be transformed into new photoproducts.

Identification of the Photoproducts. Many photoproducts of more or less large concentrations have been tentatively identified using the following.

HPLC-UV Data. Commercial 2-amino-4-methoxy-6-methyl-1,3,5-triazine (AMMT) and (2-chloroethoxy)benzene (CEBS) are representative of the two chromophoric groups present on these two SAs. Spectral data of AMMT exhibit two bands (195 and 210 nm) in the UV region, whereas those of CEBS show three bands (202, 222, and 280 nm). Therefore, the presence of benzenic groups has been easily recognizable in the photoproducts C6–C13 and T5–T10. The very close spectral data of T3 (clearly identified as the AMMT by comparison with the standard product) and C3 indicate that T3 and C3 must have nearly the same structures. C3 has thus been identified as 2-amino-4,6-dimethoxy-1,3,5-triazine. In the same way, comparison of the spectral data of CEBS with T5 and C6 has allowed us to identify T5 as 2-(2-chloroethoxy)benzenesulfonamide and C6 as the 2-(methoxyethoxy)benzenesulfonamide.

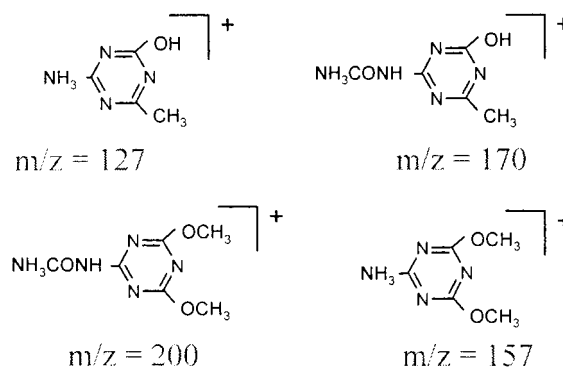
HPLC-MS Data on the Basis of Pseudomolecular Ions ($[M + H]^+$ and $[M - H]^-$) and Fragments. Photoproducts containing an unchanged triazine ring exhibit an ion fragment m/z 141 [(4-methoxy-6-methyl-1,3,5-triazin-2-yl)amino], according to results obtained by Marek and Koskinen (14). The fragment m/z 167 has been identified (14) as [(4-methoxy-6-methyl-1,3,5-triazin-2-yl)amino]carbonyl and comes from the fragmentation of photoproducts T2, T4, and T8. By analogy, a fragment at m/z 183 is obtained for CS for C2, C5, C8, C10, C11, C12, and

C13 photoproducts.



Aromatic hydroxylated photoproducts give mass spectra for which the molecular ions are 16 amu more than the parent compounds (C11, C12, C13, T9, and T10).

The following positive fragments have been identified as originating from several photoproducts



MS data are collected in **Tables 4** and **5**, whereas characteristic HPLC-UV chromatograms are presented in **Figure 4**. Several peaks of ammonium and sodium adducts were detected during analyses but have not been reported in these tables. These data allow us to propose chemical formulas as well as photodegradation schemes.

The main steps of the degradation include (cf. **Figure 5**) the cleavage of the sulfonylurea bridge to give photoproducts A (C6, T5) and B (C3, T3). This step, which corresponds to a hydrolysis mechanism, is the typical degradation pathway of SA herbicides and occurs also for chemical degradation (8). Meanwhile, at pH 7, pure chemical degradation occurs very slowly, suggesting that this hydrolysis reaction is indeed photoassisted (photohydrolysis). Products A are not represented in the kinetic photoproducts as they are rapidly photodegraded in turn. On the contrary, the concentration of B increases steadily.

Also included in degradation is the photodesulfonylation, which proceeds either by a homolytic nitrogen–sulfur cleavage or by a homolytic carbon–sulfur cleavage (a free radical mechanism). Such reactions have only been observed via photodegradation mechanisms.

Carbon–Sulfur Cleavage. The carbon–sulfur cleavage of CS and TS gives the main photoproducts C (C2 and T2) (cf. **Figure 3**, in which the C2 and T2 areas were divided by 10 and 3, respectively). In this reaction, the photogenerated sulfonyl radical ($O_2S\cdot R$) is transformed into RSO_3H . Curiously, these photoproducts have never been reported, even by Pusino et al. (15), who observed a C–S cleavage with the TS. These results, as well as the fact that these molecules are composed of two weak chromophores, suggest that the observed photoproducts depend strongly on experimental conditions. In our experiments, we have always used wavelengths >290 nm (Pusino et al. worked with lower wavelengths). This is a very important fact considering that when the UV characteristics of the C2 and T2 photoproducts (**Tables 4** and **5**) are examined, no photodegradation can be expected when $\lambda > 290$ nm, as their absorbance spectral range is far below this limit. To confirm this result, an additional experiment using a quartz photoreactor and an HPK lamp (results given elsewhere) was performed. It appears that at the very beginning of the experiment, the concentration of C increases but, after a while, decreases to zero due to the N–S bond cleavage, which yields other byproducts such as B (C3, T3) or D (C5, T4).

It is also interesting to note that ring substituents can significantly affect the photolysis reaction in terms of C–S bond stability. For example, Yang et al. (16) have found that the *o*-chloro group reinforced the photochemical stability, in terms of the C–S bond, whereas Weiss et al. (13) have found the same for the *p*-amino group, presumably because these substituents change the nature of the excitation process. This is why such a reaction does not represent an important pathway for them, but for Pusino et al. as well as for our case the *o*-O group present on the benzene ring weakens the C–S bond, which will be more easily cleaved. On the contrary, Choudhury and Dureja (4) have found this reaction to be only a minor step using chlorimuron-ethyl.

It is worthy of note that photoproducts originating from the second part of the cleavage (RO–benzene radical) have not been clearly identified, whereas Pusino et al. (15) identified one of them ($ClCH_2CH_2O-C_6H_5$) with an authentic standard. Indeed, starting from the UV spectrum, the C4 photoproduct might be one of them (in **Tables 4** and **5**, absorption peaks for benzene

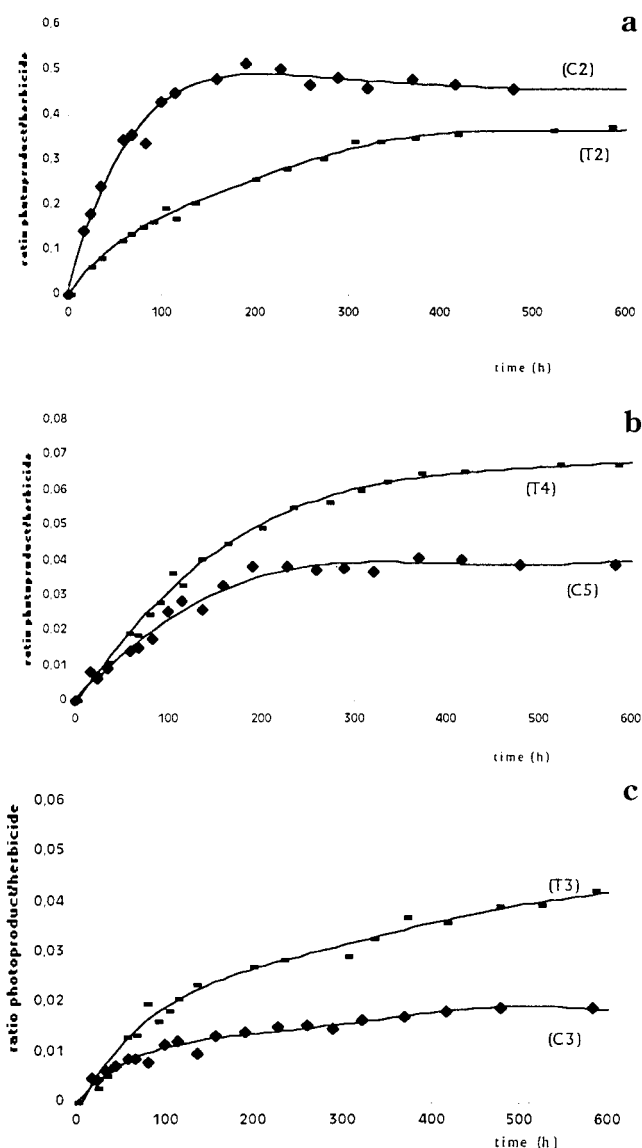


Figure 6. Comparison between the kinetic curves of the main photoproducts: (a) photoproducts C2 and T2; (b) photoproducts T4 and C5; (c) photoproducts T3 and C3.

derivatives have wavelengths higher than >270 nm), but mass spectroscopy results do not allow us a certain identification.

To summarize, we can say that the *o*-O substituent weakens the C–S bond, which can be photochemically fragmented to yield sulfonyl derivatives. The resulting photoproducts can in turn be phototransformed by an N–S cleavage into further photoproducts, if wavelengths are sufficiently energetic, for example, capable of being absorbed by the triazine cycle. Solar radiations ($\lambda > 290$ nm, 412 kJ/mol) are not sufficiently energetic to provoke this second N–S cleavage, and the sulfonyl derivative (HO_3S-R) therefore becomes the more important photoproduct.

Nitrogen–Sulfur Cleavage. In the nitrogen–sulfur cleavage, the fragmentation is followed by an H abstraction from water, which leads to photoproduct D (C4, T4). This reaction is far less important than the carbon–sulfur cleavage, as shown in **Figure 5**. Indeed, it has been shown (11) that this bond was cleaved following excitation transfer from the triazine chromophore to the sulfonylurea bridge. In our case, as the wavelengths used do not allow an efficient excitation of the triazine chromophore, it is quite normal that this reaction represents only a minor route.

The O-demethylation of the methoxy moiety of the triazine ring gives a hydroxytriazine E (C7, T7). According to the kinetic curves, its concentration increases steadily to a maximum and then decreases thereafter, meaning that these photoproducts are only intermediates and degrade further through different pathways. This step has also been observed in the case of the hydrolysis reaction (8, 17).

The O-dealkylation of lateral chains of the benzene ring leads to the products F (C8, T8). It appears that these photoproducts have never been observed by hydrolysis; these photoproducts are also intermediate species.

Comparison between the Two SAs. The two SAs differ first by the lateral chain borne by the benzene ring and second by the OCH₃ or CH₃ moieties borne by the triazine ring. These differences do not seem to overly influence quantum yield values, which are similar for both cases.

Comparison of the absorption peaks at $\lambda = 234\text{--}236$ nm in aqueous buffers showed that the molar extinction coefficient is higher for CS (**Figure 1**) than for TS. However, because the lowest wavelength used during experiments is 290 nm, it is unlikely that the photodegradation is strongly influenced.

Figure 5 shows a comparison between the kinetic curves of the main photoproducts with semiquantification obtained by expressing the ratio of photoproduct area/SA area (HPLC-UV analysis). By comparing the photoproducts C2 and T2 (**Figure 6a**) it seems that the desulfonylation via the C–S bond cleavage is more efficient for CS than for TS. As this step is the most important one, it confirms that the conversion rate for CS is faster than that for TS. On the contrary, the photohydrolysis step (**Figure 6b**, T4 and C5) and the desulfonylation one via the S–N bond cleavage (**Figure 6c**, C3 and T3) are more efficient for TS than for CS, even if at the beginning of the photoreaction, the kinetics are nearly the same. As these photoproducts are formed to a lesser extent than the C–S bond cleavage, they do not affect the values of the conversion rates too greatly.

Conclusion. This study confirms earlier findings that photodegradation can no longer be neglected for a good understanding of the evolution of environmental pollutants. We have shown in particular that their lifetimes could be much more important with regard to hydrolysis and that specific byproducts could appear.

Furthermore, the importance of the choice of the irradiation wavelength is clear. If one wishes to identify photoproducts

generated by sunlight, it is necessary to work with wavelengths >290 nm.

A complementary study using molecular modeling will be performed to better understand the photochemical behavior of SAs and also to try to forecast their photodegradation mechanisms.

LITERATURE CITED

- (1) Fredrickson, D. R.; Shea, P. J. *Weed Sci.* **1986**, *34*, 328–332.
- (2) Beyer, E. M.; Duffy, M. J.; Hay, J. V.; Schlueter, D. D. *Sulfonylureas in Herbicides: Chemistry, Degradation and Mode of Action*; Kearney, P. C., Kaufmann, D. D., Eds.; Dekker: New York, 1987; pp 117–189.
- (3) Harvey, J. J.; Dulka, J.; Anderson, J. J. *J. Agric. Food Chem.* **1985**, *33*, 590–596.
- (4) Choudhury, P. P.; Dureja, P. *J. Agric. Food Chem.* **1996**, *44*, 3379–3382.
- (5) Choudhury, P. P.; Dureja, P. *Pestic. Sci.* **1997**, *51*, 201–205.
- (6) Scrano, L.; Bufo, S. A.; Perucci, P.; Méallier, P.; Mansour, M. *Pestic. Sci.* **1999**, *55*, 955–961.
- (7) Berger, B. M.; Wolfe, N. L. *Environ. Toxicol. Chem.* **1996**, *15*, 1500–1507.
- (8) Braschi, I.; Calamai, L.; Cremonini, M. A.; Fusi, P.; Gessa, C.; Pantani, O.; Pusino, A. *J. Agric. Food Chem.* **1997**, *45*, 4495–4499.
- (9) Guitonneau, S.; Maestracci, M.; Méallier, P.; Moutié, E. *Proceedings of the XXV Congrès du Groupe Français des Pesticides*, Montpellier, France, May 17–18, 1995.
- (10) *The Pesticide Manual*, 10th ed.; Tomlin, C., Ed.; Crop Protection Publications: Cambridge, U.K. 1994.
- (11) Caselli, M.; Ponterini, G.; Vignali, M. *J. Photochem. Photobiol. A* **2001**, *138*, 129–137.
- (12) Zepp, R. G.; Cline, D. M. *Environ. Sci. Technol.* **1977**, *11*, 359–366.
- (13) Weiss, B.; Durr, H.; Haas, H. *J. Angew. Chem., Int. Ed. Engl.* **1980**, *19*, 648–649.
- (14) Marek, L.; Koskinen, W. *J. Agric. Food Chem.* **1996**, *44*, 3878–3881.
- (15) Pusino, A.; Braschi, I.; Petretto, S.; Gessa, C. *Pestic. Sci.* **1999**, *55*, 479–481.
- (16) Yang, X.; Wang, X.; Kong, L.; Wang, L. *Pestic. Sci.* **1999**, *44*, 751–754.
- (17) Sarmah, A. K.; Kookana, R. S.; Duffy, M. J.; Alston, A. M.; Harch, B. D. *Pest. Manag. Sci.* **2000**, *56*, 463–471.

Received for review July 20, 2001. Revised manuscript received November 14, 2001. Accepted November 14, 2001.

JF010948S